Revealing and resolving the restrained enzymatic cleavage of DNA self-assembled monolayers on gold: electrochemical quantitation and ESI-MS confirmation

Xiaoyi Gao,[†] Mingxi Geng,[†] Yunchao Li[*,†], Xinglin Wang,[†] and Hua-Zhong Yu[*,‡]

[†]*Department of Chemistry, Beijing Normal University, Beijing 100875, P. R. China*

[‡]*Department of Chemistry, Simon Fraser University, Burnaby, British Columbia V5A 1S6, Canada*

* Corresponding authors: liyc@bnu.edu.cn,+86-10-5880-4077 (Y.L.); hogan_yu@sfu.ca, +1-778-782-8062 (H.Y.)

ABSTRACT: Herein we report a combined electrochemical and ESI-MS study of the enzymatic hydrolysis efficiency of DNA self-assembled monolayers (SAMs) on gold, platform systems for understanding nucleic acid surface chemistry and for constructing DNA-based biosensors. Our electrochemical approach is based on the comparison of the amounts of surface-tethered DNA nucleotides before and after Exonuclease I (Exo I) incubation using electrostatically bound $[Ru(NH_3)_6]^{3+}$ as redox indicators. It is surprising to reveal that the hydrolysis efficiency of ssDNA SAMs does not depend on the packing density and base sequence, and that the cleavage ends with surface-bound shorter strands (9-13 mers). The ex-situ ESI-MS observations confirmed that the hydrolysis products for ssDNA SAMs (from 24 to 56 mers) are dominated with 10-15 mer fragments, in contrast to the complete digestion in solution. Such surface-restrained hydrolysis behavior is due to the steric hindrance of the underneath electrode to the Exo I/DNA binding, which is essential for the occurrence of Exo I-catalyzed processive cleavage. More importantly, we have shown that the hydrolysis efficiency of ssDNA SAMs can be remarkably improved by adopting long alkyl linkers (locating DNA strands further away from the substrates).

Keywords: Exo I, DNA self-assembled monolayers, DNA cleavage, electrochemical analysis, ESI-MS

INTRODUCTION

Exonuclease I (Exo I) from E.coli is an Mg^{2+}-dependent monomeric enzyme, which typically takes a C-shape morphology with three distinct domains.[1-3] It is known for its high specificity for progressively cleaving single-stranded DNA (ssDNA) from 3' to 5'-end and releasing 5'-phosphate mononucleotides in a stepwise manner. The Exo I catalyzed hydrolysis requires the presence of free 3'-hydroxyl terminus for the digestion of ssDNA and does not show any activity to either double-stranded DNA (dsDNA) or to ssDNA with 3'-modification.[4-6] Benefited from this unique property, Exo I has been extensively employed in nucleic acid biochemistry and genetic engineering, such as DNA mutation repair/avoidance,[7] PCR primer digestion,[8] and DNA demethylation detection.[9]

Recently, Exo I has been creatively introduced to and popularly utilized in the fabrication of biosensors as an effective tool for improving their sensitivities and selectivities.[10-24] For example, Jiang and co-workers developed a universal Exo I-assisted terminal protection protocol for detecting various targets of interest.[25] Taking advantage of Exo I-assisted background reduction and signal amplification capability, Wang et al.[26, 27] and Xiang et al.[28, 29] were able to detect pM-levels of thrombin in human serum and folate receptor in buffer, respectively. The above-mentioned Exo I-assisted signal enhancement strategies are based on the assumption that Exo I can cleave surface-tethered ssDNA efficiently and completely. However, for chip-based DNA reactions the steric effects from neighboring DNA strands and the underneath substrate are typically prominent. In consideration of such blocking effect, the Exo I-catalyzed hydrolysis behavior of surface-immobilized ssDNA is likely different from that of solution-dispersed ssDNA. Fojta et al. previously reported that the restricted accessibility of another enzyme, deoxyribonuclease I to the surface-confined DNA leads to sluggish hydrolysis kinetics of DNA on electrode surface.[30] Consequently, we can speculate that the Exo I-based biosensors may lose their detection sensitivity and even entire function in particular cases; the DNA/RNA biosensors based on Exo I-assisted terminal protection strategy often have their signal reporting domains situated in the close proximity of the substrates.[17,18] If single-stranded DNA probes cannot be cleaved completely by Exo I, their residues may interact with the reporter DNA and cause false-positive signals. Until now, only limited efforts have been devoted to understand the degradation

of surface-tethered ssDNA by Exo I, although such behavior is critical to the signal detection/amplification performance of Exo I-based DNA biosensors. Therefore, it is imperative to investigate the mechanism of Exo I-induced hydrolysis of DNA self-assembled monolayers (SAMs) on gold, the general platform for the creation of DNA-based biosensors.

It is technically challenging to evaluate the Exo I-catalyzed hydrolysis behavior of surface-tethered ssDNA, as the most common methods, such as gel electrophoresis, radio-isotope labeling, mass spectrometry, are time-consuming and unsuitable for in-situ monitoring the rapid mass or length changes of DNA strands immobilized on a solid substrate. In the meantime, electrochemical methods, such as cyclic voltammetry (CV) and electrochemical impedance spectroscopy (EIS) have been successfully adopted to study site-specific DNA cleavage by EcoRI endonuclease.[31] In retrospect, both CV and chronocoulometry (CC) are well-known electrochemical methods for measuring the surface density of DNA strands immobilized on electrode.[32, 33]

In this paper, we adapt a simple and efficient electrochemical method (i.e., CV quantitation protocol) to evaluate the cleavage behavior of Exo I to ssDNA self-assembled monolayers (SAMs). By comparing the amount of DNA nucleotides tethered on electrode before and after Exo I-catalyzed cleavage using $[Ru(NH_3)_6]^{3+}$ as redox indicators, the hydrolysis efficiency as well as the residue products can be evaluated. We start this study with a systemic investigation of the dependence of cleavage efficiency on surface density, length, and sequence of surface-tethered DNA single strands, followed by confirmation of the hydrolysis products based on ex-situ ESI-MS measurements. As described below, we were able to reveal the mechanism of the surface-restrained enzymatic cleavage of DNA SAMs on gold, which can be resolved by adopting long linkers to locate DNA strands further away from the substrate.

EXPERIMENTAL SECTION

Materials and reagents. Magnesium chloride hexahydrate, sodium chloride, sodium carbonate anhydrous, sodium thiosulfate pentahydrate, sulphuric acid (95–98%), hydrochloric acid (37%), ethanol ($\cong$ 99.7%), and nitric acid (>90%) were purchased from Beijing Chemical Reagent Co.

(Beijing, China). Tris (hydroxymethyl)-aminomethane, Tris (hydroxymethyl-aminomethane hydrochloride (Tris-HCl) and 6-mercapto-1-hexanol (MCH) were ordered from Sigma-Aldrich (Saint Louis, USA). Hexaammineruthenium (III) chloride (98%), Tris- (2-carboxyethyl) phosphinehydrochloride (TCEP), formaldehyde, and silver nitrate were purchased from Acros (Brussels, Belgium). Exo I and Alkaline Phosphatase were purchased from the Thermo Scientific (Lithuania).

All oligonucleotides (sequences listed in **Table 1**) were of HPLC grade and obtained from Sangon Biotechnology Inc. (Shanghai, China). The oligonucleotide stock solutions (100 µM) and buffer solutions were prepared in deionized water (≥18.2 MΩ cm) produced from a Barnstead Easypure System (Thermo Scientific Inc., Dubuque, USA). Unless otherwise indicated, all other reagents and solvents were purchased in analytical grade and used without further purification.

Table 1. Oligonucleotide sequences of ssDNA used in Exo I-assisted hydrolysis assays.

DNA strand	Sequence	MW(Da)
ssDNA-12	HS-$(CH_2)_6$-O-5'- ACA CGC TCA CTA -3'	3707
ssDNA-24	HS-$(CH_2)_6$-O-5'- ACA CGC TCA CTA TCA CAA ACA GCT -3'	7368
ssDNA-48	HS-$(CH_2)_6$-O-5'- ACA CGC TCA CTA TCA CAA ACA GCT GGA AAC GCT CAC CAT CAC TAT CTA -3'	14696
ssDNA-56	HS-$(CH_2)_6$-O-5'- ACA CGC TCA CTA TCA CAA ACA GCT GGA AAC GCT CAC CAT CAC TAT CTA ACA CGC TC -3'	17112
ssDNA-24CA	HS-$(CH_2)_6$-O-5'-CAC ACA CAC ACA CAC ACA CAC ACA-3'	7230
ssDNA-48CA	HS-$(CH_2)_6$-O-5'-CAC ACA CAC ACA CAC ACA CAC ACA CAC ACA CAC ACA CAC ACA CAC ACA -3'	14529
C18ssDNA-48	HS-**$(CH_2)_{18}$**-O-5'-ACA CGC TCA CTA TCA CAA ACA GCT GGA AAC GCT CAC CAT CAC TAT CTA -3'	15391
C30ssDNA-48	HS-**$(CH_2)_{30}$**-O-5'-ACA CGC TCA CTA TCA CAA ACA GCT GGA AAC GCT CAC CAT CAC TAT CTA -3'	15655

Polyacrylamide gel electrophoresis (PAGE) assay. A 20% native polyacrylamide gel was prepared using $1\times$ TB buffer (89 mM Tris–borate, pH 8.3). Each sample contained 10 μM ssDNA (ssDNA-48). The gel was run at 100 V for 90 min in $1\times$ TB buffer. After electrophoresis, the gel was immersed in a stains-all solution (0.4 g of silver nitrate, 300 μL of formaldehyde, 200 mL of H_2O) for 30 min. Subsequently, the gel was incubated in the colorimetric solution (6.0 g of sodium carbonate anhydrous, 300 μL of formaldehyde, 40 μL of sodium thiosulfate of 10 mg/ml, 200 mL of H_2O) for 5 ~10 min. Finally, the PAGE results were photographed using a digital camera.

Preparation of DNA-modified gold electrodes. Gold disk electrodes (2.0 mm in diameter) were polished with 0.3 μm Al_2O_3 powder and rinsed with plenty of deionized water and anhydrous ethanol, respectively. Afterwards, they were electrochemically cleaned in 1.0 M H_2SO_4 solution by scanning potential between -0.2 and 1.6 V (vs. Ag|AgCl) until a reproducible CV was obtained. The cleaned electrodes were rinsed thoroughly with deionized water and finally blown dry with high-purity nitrogen before DNA adsorption. The thiolated ssDNA (freshly prepared) of different concentrations in 10 mM Tris coupling buffer (containing 150 mM NaCl, 50 mM $MgCl_2$, pH $= 7.4$ at 25 °C) were heated at 80 °C for 5 min followed by slowly cooling to room temperature. The cleaned electrodes were immersed in 100 μL of thus prepared thiolated ssDNA solution in 10 mM Tris coupling buffer for 4.0 h. After immobilization, they were rinsed with Tris buffer, and then incubated in 1.0 mM MCH for 1.0 h, and thoroughly rinsed again with Tris buffer before electrochemical measurements.

Electrochemical characterizations. Cyclic voltammograms (CVs) were recorded on a Zahner Zennium electrochemical workstation with a conventional three-electrode cell consisting of an Ag/AgCl/3.0 M NaCl reference electrode, a platinum counter electrode, and a gold working electrode (modified with ssDNA/MCH). All measurements were performed at room temperature in 10 mM Tris buffer (pH 7.4) containing 5.0 μM $[Ru(NH_3)_6]Cl_3$. The electrolyte solutions were deoxygenated with N_2 for 12 min prior to measurement and kept under N_2 atmosphere throughout the measurements. The cathodic peak of the first scan was integrated to estimate the amount of ssDNA on the electrode.[32]

Cleavage of ssDNA by Exo I. The enzyme solution contained 1.25 U/μL Exo I (unless otherwise stated) was prepared in a buffer of 67 mM glycine-KOH (pH 9.5), 67 mM $MgCl_2$ and 10 mM DTT. To

cleave ssDNA in solution, 2.0 μL of 10 μM ssDNA was added into 18 μL of the enzyme solution and

incubated at 37 °C for 30 min. For surface experiments, the ssDNA-modified gold electrodes were

immersed in 80 μL of enzymatic reaction solutions at 37 °C for 12 h (unless otherwise stated).

Electrospray Ionization-Mass Spectrometry (ESI-MS) Measurements. After enzymatic

cleavage, the hydrolysis products were removed electrochemically from the electrode surface (biased

-1.2 V for 4 min);[36] the products from ca.45 electrodes were collected together and freeze-dried for the

MS measurements. The ESI-MS spectra were obtained with a Finnigan LCQ Deca XP Plus ion rap

mass spectrometer (San Jose, CA). Before testing, the sample was re-dissolved in deionized water

containing 10% trimethylamine (v/v) with final a concentration at nM level. The electrospray source

was set at 2.5 kV spray voltage and 120 °C capillary temperature. The spectral were acquired in the

negative ionization mode and analyzed using ProMass Deconvolution™ Software.

RESULTS AND DISCUSSION

Exo I-catalyzed cleavage of ssDNA in solution. It is generally accepted that Exo I catalyzes the

cleavage of ssDNA from 3'-terminus in a highly processive manner.[1,4] Before the study on electrode

surface, we have run polyacrylamide gel electrophoresis assays to examine the ssDNA residues upon

Exo I catalyzed hydrolysis in solution. As shown in Figure 1(a), a clear band was observed on Lane 4,

where the ssDNA-48 strands were not subjected to Exo I treatment. The band became dimmer with

increased concentration of Exo I (Lane 5 to 9). When the concentration reaches 0.5 U/μL, the original

band essentially disappeared. Meanwhile, no bands corresponding to fragments beyond 5-mer strands

were observed, suggesting that solution-dispersed ssDNA can be hydrolyzed completely (at least the

major products are not longer than 5-mer strands) with sufficient amount of Exo I.

The hydrolysis products of solution-dispersed ssDNA were also examined by ESI-MS, a gold

standard for oligo analysis. As depicted in Figure 1(b), after ssDNA-48 treated with Exo I, the original

strong single peak at 14,696 Da (48 mer) was completely diminished, while multiple peaks

corresponding to much shorter oligoes (from 3-mer to 8-mer) were evident. The signal intensity of the

most abundant peak (1,583.6 Da, 5-mer) is only account for 1.5% of the original ssDNA-48 peak.

These results confirm that the majority of ssDNA-48 strands were hydrolyzed by Exo I as indicated by the gel electrophoresis studies. The very low abundance of the residue oligo fragments in the MS spectrum (Figure 1b) also explains the fact that we did not observe any bands (below 10 mer) in the gel experiments (Figure 1a).
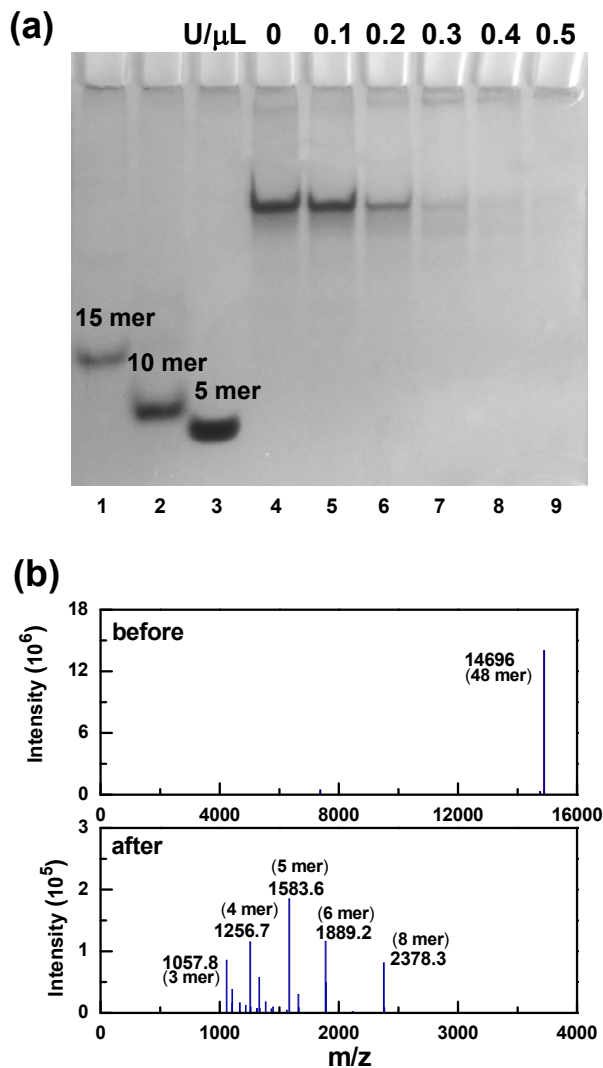

Figure 1. (a) Photo of the silver-stained native polyacrylamide gel showing the hydrolysis results of ssDNA-48 treated with Exo I for 30 min at 37 °C. Lane 1 to 3: DNA markers (15, 10, 5 mer); Lane 4-9: 10 µM ssDNA-48 with adding different concentrations of Exo I (0, 0.1, 0.2, 0.3, 0.4, and 0.5 U/µL, respectively). (b) ESI-MS spectra of ssDNA-48 before and after hydrolysis with Exo I for 30 min at 37 °C.

Quantitation of the hydrolysis efficiency of Exo I for surface-immobilized ssDNA. To quantitatively determine the cleavage efficiency of Exo I to ssDNA SAMs on gold, a simple and rapid,

voltammetric method based on the quantitation of electrostatically bound redox cations (e.g., $[Ru(NH_3)_6]^{3+}$) was proposed (Scheme 1). In the past, this method has been widely used for determining the surface density of DNA strands immobilized on electrode surface, with the assumption that the negative charges on DNA phosphate backbones are solely compensated by multiply charged $[Ru(NH_3)_6]^{3+}$ cations.[32-33] The number of DNA strands per unit area (Γ_{DNA}) immobilized on an electrode can be determined from the surface density of surface-bound redox cations (Γ_{Ru}), which is calculated from the integrated charge of the cathodic peak (i.e., the reduction of $[Ru(NH_3)_6]^{3+}$).

$$\Gamma_{Ru} = Q/nFA \qquad (1)$$

$$\Gamma_{DNA} = \Gamma_{Ru}(z/m)N_A \qquad (2)$$

where n is the number of electrons involved in the redox reaction, F is Faraday's constant, A is the electrode area, z is the valence of the redox cation, m is the number of nucleotides in the DNA strands, and N_A is the Avogadro constant.
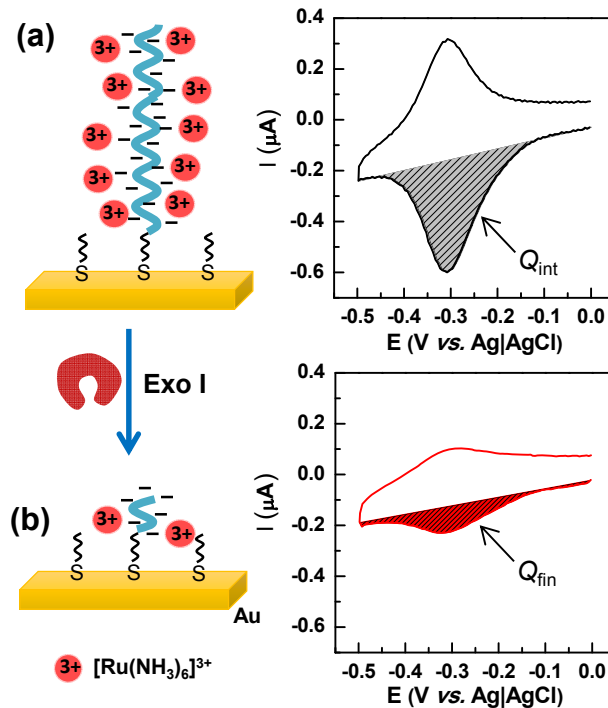
Scheme 1. Principle of the electrochemical protocol for quantifying the efficiency of Exo I catalyzed hydrolysis of ssDNA SAMs. The right insets show the CV response of 5.0 μM $[Ru(NH_3)_6]^{3+}$ on gold electrodes modified with ssDNA-48 in 10 mM Tris buffer before (top) and after (bottom) undergoing Exo I incubation for 12 h. The scan rate was 50 mV/s.

The efficiency of Exo I-catalyzed hydrolysis of ssDNA SAMs on gold can be calculated using the following equation:

$$\text{Hydrolysis Efficiency (HE\%)} = (Q_{int} - Q_{fin})/Q_{int} \times 100\% \tag{2}$$

where Q_{int} and Q_{fin} are the integrated charges before and after the Exo I catalyzed hydrolysis, respectively. As expected (Scheme 1, right top inset), a pair of clear-cut CV peaks for the $[Ru(NH_3)_6]^{3+}$ /$[Ru(NH_3)_6]^{2+}$ redox process on DNA SAM-modified gold electrode was observed; upon hydrolysis, the peaks became much smaller. In combination with the subsequent ESI-MS analysis of the hydrolysis products, we should be able to provide a better understanding of the hydrolysis process of ssDNA SAMs on gold.

With the above mentioned protocol, we systemically tested the effects of Exo I concentration and reaction time applied in surface-confined ssDNA hydrolysis assay. As shown in Figure 2(a), the cathodic peak of $[Ru(NH_3)_6]^{3+}$ decreases with the concentration of Exo I increased from 0.25 to 2.5 U/μL, suggesting that ssDNA strands on electrode were not cleaved to the same extent. The results shown in Figure 2(b) confirm that the hydrolysis efficiency is highly dependent on the Exo I concentration; in the range from 0.04 to 1.25 U/μL the hydrolysis efficiency improves linearly, but levels off when the Exo I concentration increased to 1.25 U/μL. With the "adequate" concentration of Exo I, the influence of incubation time on the hydrolysis efficiency was examined subsequently. The observed cathodic peak of $[Ru(NH_3)_6]^{3+}$ gradually decreased with increasing the incubation time from 30 min to 3.0 h, and then remained constant thereafter (Figure 3(a)). The relationship between hydrolysis efficiency and the reaction time shown in Figure 3(b) indicates rather sluggish hydrolysis kinetics. It took about 3.0 h for the Exo I to hydrolyze the surface-immobilized ssDNAs under the set experimental conditions, which is much longer than that for hydrolyzing solution-dispersed ssDNA (30 min). Unlike the solution experiments, the maximum hydrolysis efficiency is around 67% in both the concentration and reaction time tests (Figure 2b and Figure 3b), i.e., increased concentration of Exo I or prolonged incubation time does not help to completely cleave the DNA strands immobilized on gold surfaces.
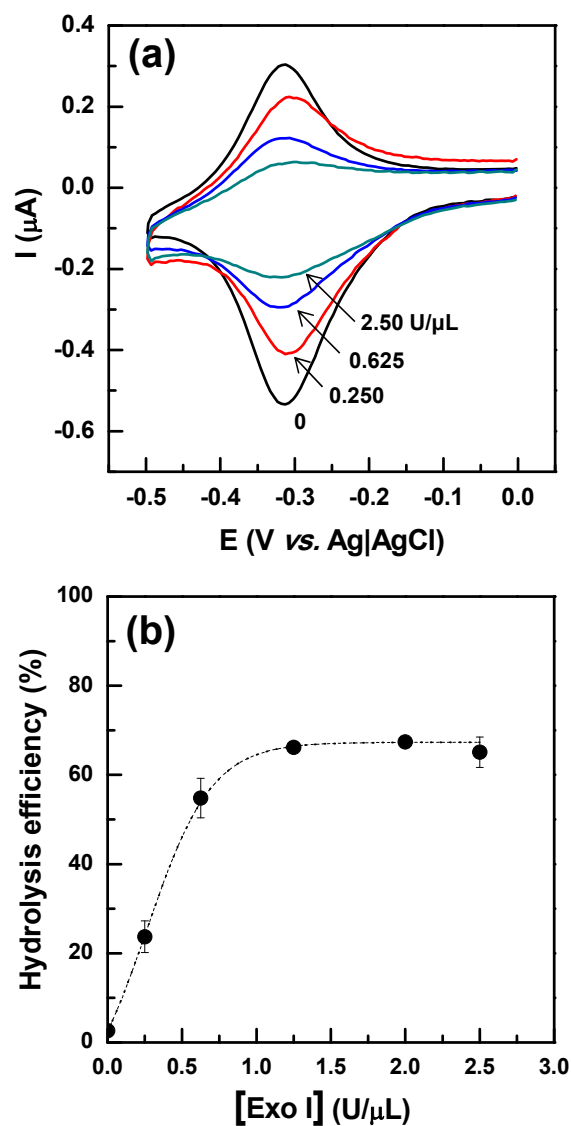
Figure 2. (a) CV responses of 5.0 µM $[Ru(NH_3)_6]^{3+}$ on gold electrodes modified with ssDNA-48 in 10 mM Tris buffer at a scan rate of 50 mV/s upon incubation with different concentrations of Exo I. The incubation time was kept for 12 h in all cases. (b) Hydrolysis efficiency of surface-tethered ssDNA as a function of the Exo I concentration. The data are extracted from (a) and Table S1 (Supporting Information), which showing standard deviations of three replicated measurements.
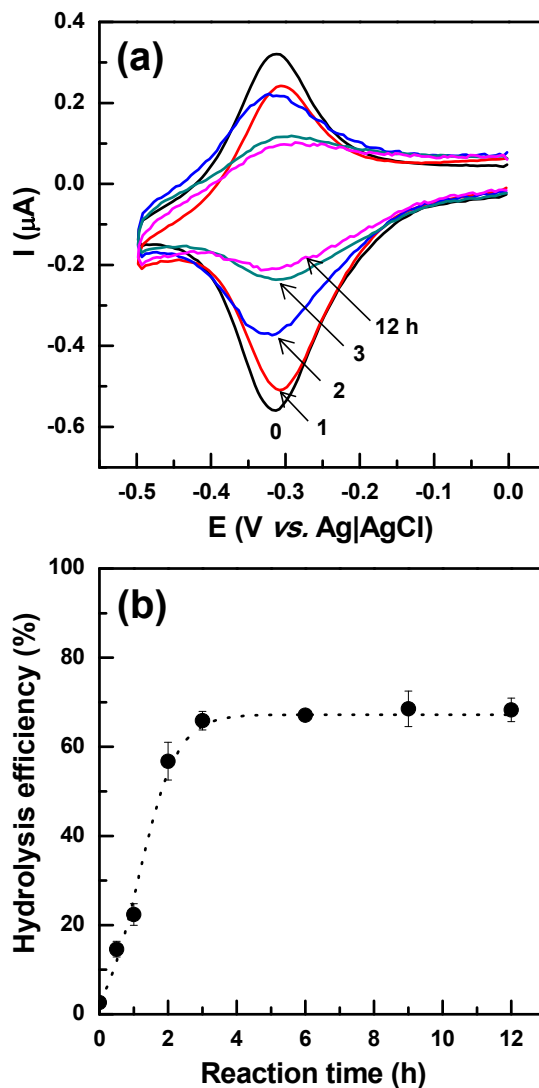
Figure 3. (a) Representative CV response of gold electrodes modified with ssDNA-48 SAMs in 10 mM Tris buffer at in presence of 5.0 µM $[Ru(NH_3)_6]^{3+}$; the electrodes were subjected to 1.25 U/µL Exo I and incubated for different period of time, and the scan rate was 50 mV/s. (b) Hydrolysis efficiency as a function of Exo I incubation time. The data are extracted from (a) and Table S2 (Supporting Information), which represent the average of three replicated measurements.

To better understand such an incomplete cleavage behavior, we systemically studied the correlation between the cleavage efficiency and the surface density of ssDNA SAMs on gold, a key factor governing the surface-related reactions in many cases.[34,35] Figure 4(a) shows the representative

CV curves of the surface-confined ssDNA-48 with high, medium, and low surface density before and after incubation with 1.25 U/ µL Exo I for 12 h at 37 °C. The cathodic peaks in all three cases substantially decreased but did not totally diminish, indicating that a portion of ssDNA strands remained on the gold electrode. It is surprising to notice that the hydrolysis efficiency stays almost the same in the entire range of varied surface densities (Figure 4(b)). Such a surface density-independent hydrolysis behavior indicates that the spatial steric effect among DNA chains is not responsible for the incomplete hydrolysis (*vide infra*).

Other factors may influence the hydrolysis efficiency include the length and sequence of the surface bound ssDNA strands. In Figure 5, we have plotted the HE% values for two other ssDNA SAMs; one with a much shorter length (24 mer), the other is longer (56 mer). In both cases the hydrolysis efficiency does not depend on the surface density in a broad range, although the values seem to be lower at low surface densities for the 24 mer. The other observation is that the averaged HE% values for the three ssDNA SAMs (24, 48, and 56-mer) being studied are distinctly different. A decreasing trend was observed with shortened DNA strands, i.e., the SAMs with ssDNA-24 has the lowest hydrolysis efficiency (Figure 5). We have also discovered that repeated hydrolysis, i.e., replacing the enzyme solution every 3 h, improves the efficiency slightly. The highest achievable hydrolysis efficiency (HE%) values of the three ssDNA SAMs (24, 48, 56-mer) by Exo I are 55.5 ± 4.3%, 77.3 ± 4.5%, and 78.7 ± 2.4%, respectively. Assuming that all DNA strands on the surface are cleaved to the same length, the corresponding hydrolysis products of 24, 48 and 56-mer samples should be 10-12 mer, 9-13, and 11-13 mer, respectively (Table 2).

To confirm the above results, we have also carried out chronocoulometry studies to evaluate the hydrolysis efficiency, which is consistent with CV observations (Supporting Information). In a different set of experiments, ssDNA SAMs with different base sequences (repeated CA) were chosen to examine the effect of nucleotide sequence to the Exo I-catalyzed hydrolysis efficiency. As shown in Figure S3 in Supporting Information, our results confirmed that the nucleotide sequence has no effect on the incomplete cleavage behavior.
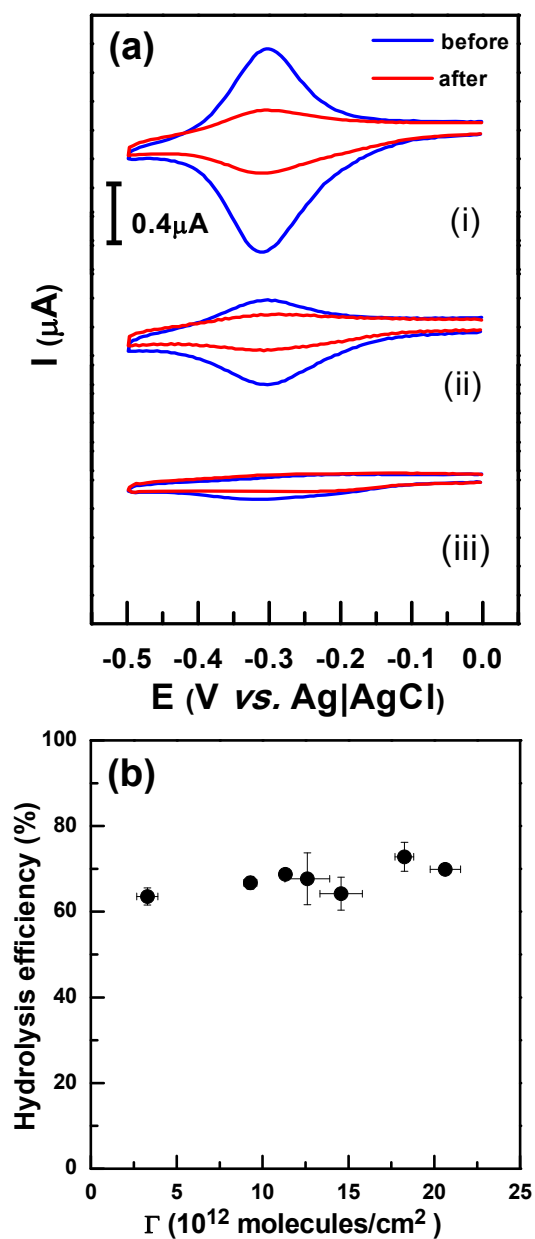
Figure 4. (a) Representative CV responses of gold electrodes modified with high (i), medium (ii) and low (iii) density of ssDNA-48 in 10 mM Tris buffer in the presence of 5.0 µM $[Ru(NH_3)_6]^{3+}$ before and after digesting with 1.25 U/µL Exo I for 12 h. The scan rate was 50 mV/s for all cases. (b) Hydrolysis efficiency as a function of the surface density. The error bars shown in (b) are from three replicated experiments.
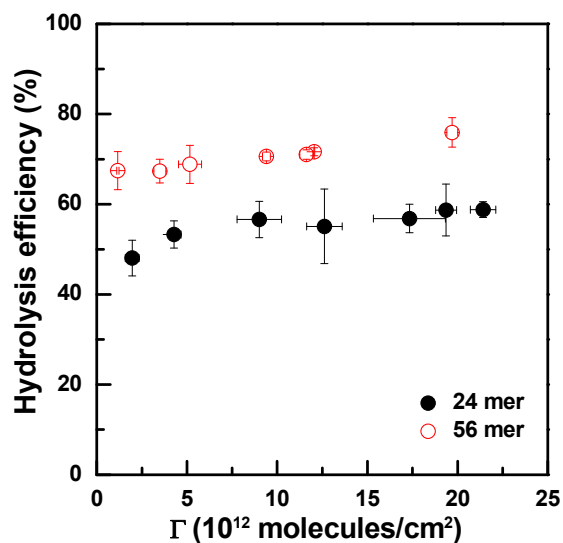
Figure 5. Hydrolysis efficiency comparison of surface-tethered ssDNA of different chain lengths.

To validate the electrochemical observation, we also carried out ESI-MS to examine the DNA fragments (removed electrochemically from the electrode surfaces).[36] Although the signals obtained are rather weak (due to the difficulty in collecting samples), these measurements provided unequivocal identification of the hydrolysis products. As shown in Figure 6 and Figure S4, the peaks corresponding to the original ssDNA strands all disappeared upon hydrolysis, which ruled out the possibility of cleaving a portion of surface-bound strands (i.e., "uneven cut" of ssDNA SAMs on gold). More importantly, even with low signal intensity, multiple mass peaks were clearly observed in a much lower mass range (~3000 Da); the peaks with relatively high abundance (≥ 10%) are corresponding to DNA strands of 11-15 mers, which are apparently longer than the oligo residues formed in solution-based hydrolysis. The significance is that the EIS-MS determined fragment lengths are in general agreement with the electrochemical results reported above (Table 2). The combined electrochemical and ESI-MS studies confirms that Exo I-catalyzed hydrolysis of ssDNA SAMs is not complete, and that the residue DNA strands are of similar length (from 10 to 15 mer). In a subsequent control experiment, we also unveiled that Exo I showed very limited effect to hydrolyze 12-mer ssDNA SAMs (Figure S5 in Supporting Information). This provides an unequivocal evidence for the difficulty of hydrolyzing 12-mer (and shorter) DNA strands on surface. Beyond the difficulty in interpreting the relative abundance of the MS peaks, the residue strands predicted with electrochemical data are in good agreement.
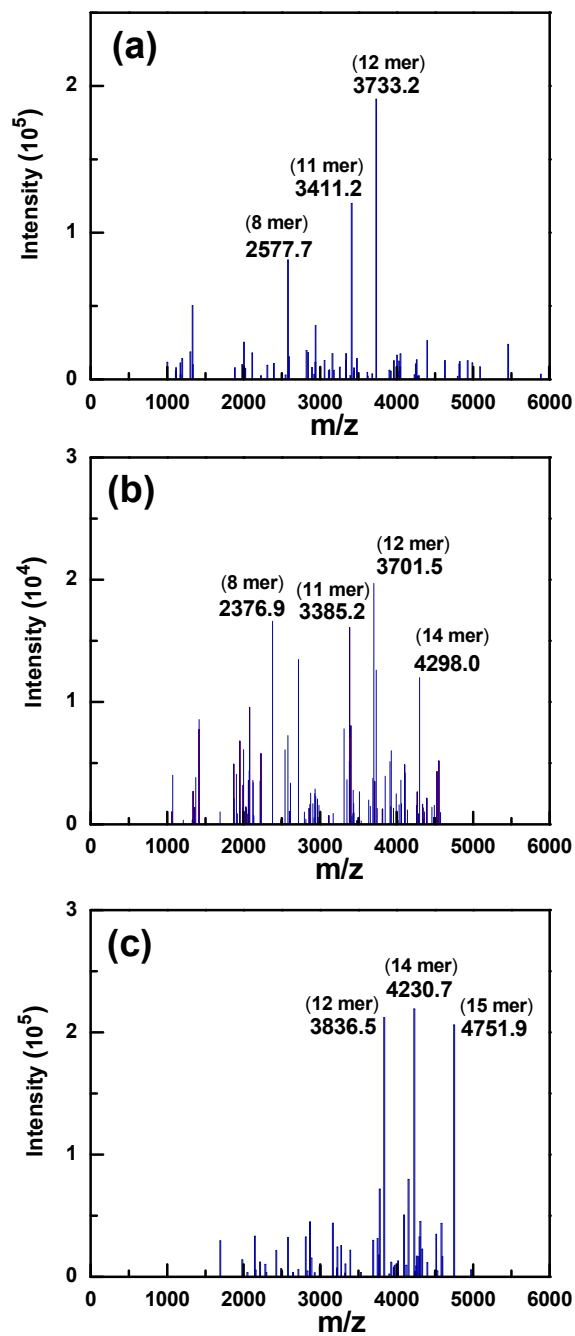
Figure 6. ESI-MS spectra ssDNA-24 (a), ssDNA-48 (b), and ssDNA-56 (c) after hydrolysis with 1.25 U/μL Exo I at 37 °C for 12 h. The hydrolyzed DNA strands were removed from electrode surface by electrochemical reduction method,[36] and samples of multiple electrodes (> 40) were combined to achieve detectable concentrations.

Table 2. Comparison the length of hydrolysis fragments of the surface-tethered ssDNA measured by CV and MS.

Original ssDNA	Fragments predicted with CV data (mer)	Fragments determined by ESI-MS (mer)
ssDNA-24	10-12	10(w), 11(w), 12 (s)
ssDNA-48	9-13	11 (s), 12 (s); 14 (w)
ssDNA-56	11-13	12 (s); 14 (s); 15 (s)

* s indicates the strong peaks; w refers to other detectable peaks. The residue DNA fragments predicted with CV data are based on the changes in Γ_{Ru} (Eqs. 1-2), assuming that all strands are cleaved to the same length.

Mechanistic illustration and the solution thereof. Based on experimental observations above, two conclusions are apparent regarding the Exo I catalyzed hydrolysis of ssDNA SAMs on gold: (1) the process is not complete and the efficiency does not depend on the surface density or the sequence of DNA strands; (2) the residue strands have similar lengths (10-15 mers), which are independent of the original DNA strands. These residue strands are much longer than those of solution-dispersed ssDNA experiments.[6] It is well known that on-chip reactions are typically subjected to the steric effects among DNA strands, however, the spatial restrictions in the vertical direction has been generally ignored. Since the DNA surface density does not influence the final hydrolysis efficiency, we thus speculate that the restriction is likely due to the steric hindrance between the rather large enzyme (Exo I) and the gold electrode. In fact, previous studies have revealed that each Exo I molecule has two binding sites contributing to its processive cleavage capability.[3,6,37] One is termed as the "active site", which is responsible for hydrolyzing DNA nucleotide; the other is referred as the "anchor site", which ensures its binding with DNA tightly. The two functional sites are located at the bottom and top of its central groove respectively. The central groove itself is about 5 nm long, which accommodates 12-mer nucleotides of ssDNA.[2,37] In this context, Exo I can hydrolyzes surface-confined ssDNA progressively until reaching the underneath substrate (Scheme 2). Under this situation, Exo I is no longer able to translocate along the DNA single strand, and the length of residue strands would be ~12 mer, ca. 5.0 nm

including the linker.[38,39] This means that the restricted accessibility of Exo I to the DNA nucleotides on surface contributes to the limited hydrolysis efficiency.
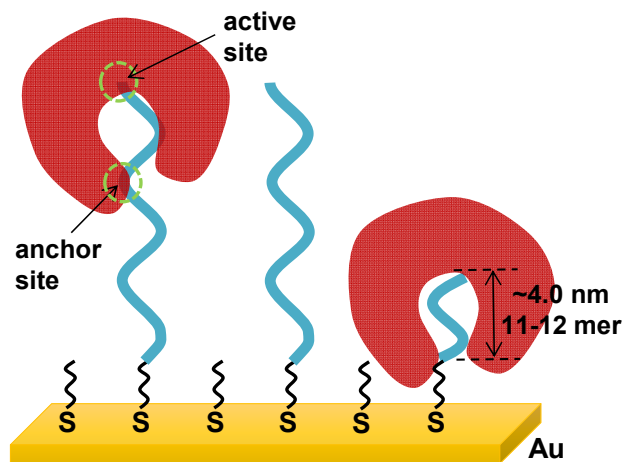
Scheme 2. Schematic view of the restricted cleavage behavior of Exo I toward ssDNA SAMs on gold; the size of the Exo I and DNA strands are not drawn to the scale.

The above findings remind us that we should consider the incomplete cleavage of surface-confined ssDNA when treated with Exo I in order to fully utilize its unique catalytic hydrolysis function for chip-based sensor design. An apparent solution to improve the Exo I-catalyzed hydrolysis efficiency toward ssDNA SAMs, is to adapt a longer linker, by which ssDNA strands can be moved away from the electrode surface. The effect of the different spacers on the immobilization degree and on the consecutive hybridization efficiency/kinetics of DNA strands on both polymeric and gold substrates have been studied previsously,[41-42] which is different from the objective in this study. Depicted in Figure 7(a), we have utilized ssDNA strands modified with different lengths of methylene linkers (C_6, C_{18} and C_{30}) to adjust the distance between DNA and the underneath gold surface. The acquired CV responses (Figure 7a) showed significant improvement with increasing the ssDNA linker length. Particularly, when cleaving the ssDNA of C_{30} linker (the linker length is about 5.0 nm), the cathodic peak was found to be close to that of a "bare electrode". In this case, the surface is only modified with MCH only, and the solution- diffused $[Ru(NH_3)_6]^{3+}$ did not produce significant faradic signals.
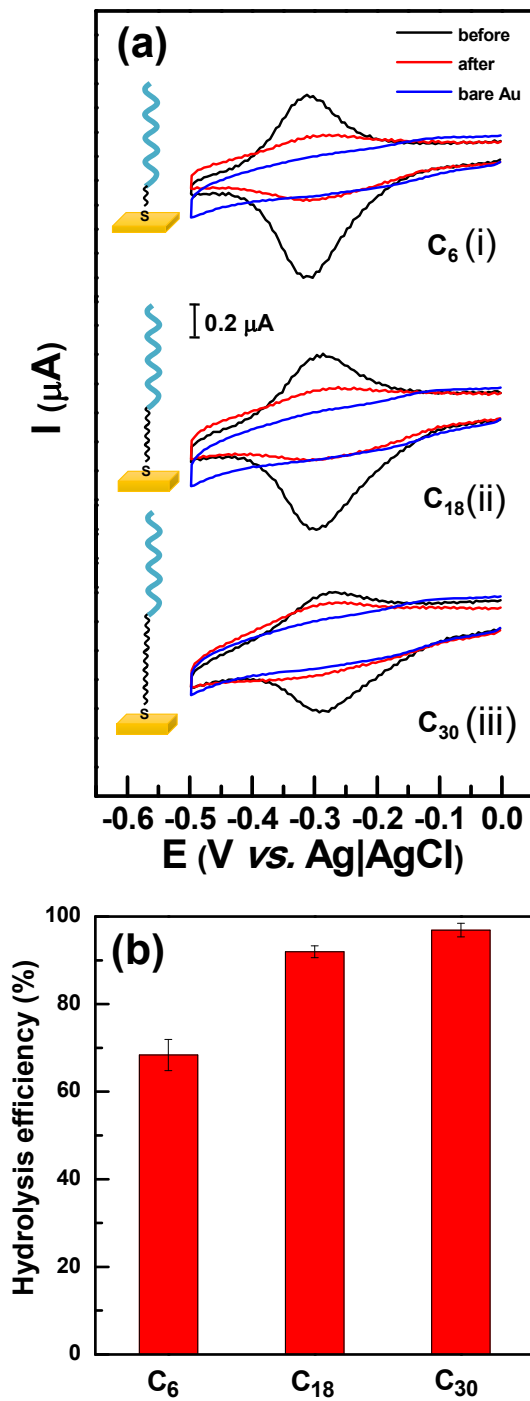
Figure 7. (a) CV responses of gold electrodes modified with ssDNA-48 of C_6 (i), C_{18} (ii) and C_{30} (iii) linker in 10 mM Tris buffer in the presence of 5.0 μM $[Ru(NH_3)_6]^{3+}$ at a scan rate of 50 mV/s before and after treating with 1.25 U/μL Exo I for 12 h. (b) Comparison of the hydrolysis efficiency of the surface-tethered ssDNA-48 of different linker lengths.

This result suggests a complete removal of the ssDNA strands from the electrode upon incubation with Exo I. The calculated hydrolysis efficiencies are plotted in Figure 7(b), which shows the hydrolysis efficiency was improved from ca 70% to $96 \pm 2\%$ as the linker length increases from 6 to 30 methylene groups. Based on above results, we are able to conclude that the incomplete cleavage issue of Exo I to surface-tethered ssDNA can be fully solved by adopting a longer linker for preparing ssDNA SAMs.

CONCLUSION

In summary, with a simple, rapid electrochemical approach the efficiency of enzymatic hydrolysis of ssDNA SAMs can be determined. Particularly, our finding revealed that the hydrolysis efficiency of Exo I toward ssDNA SAMs on gold is independent of the surface densities and sequences. The combined electrochemical and ESI-MS studies confirmed a surprising, incomplete hydrolysis behavior of Exo I toward surface-immobilized ssDNA, i.e., 10~15-mer DNA strands were remained on the electrode, which is independent of the original DNA lengths. Such incomplete hydrolysis behavior of Exo I is due to the steric hindrance between the electrode and the enzyme, which is inevitable for chip-based biosensors, but can be overpassed by adopting longer linkers for preparing DNA SAMs. It should emphasized that the better understanding of the Exo I catalyzed cleavage behavior will certainly help to design a variety of DNA-based biosensors and devices with improved the sensitivity and specificity.

## Acknowledgements

Supporting Information

Additional experimental results including chronocoulometry studies of the hydrolysis of ssDNA SAMs and the comparison with CV data, ESI-MS confirmation of the hydrolysis residues of ssDNA-48 SAMs, CV studies of the hydrolysis of ssDNA SAMs with repeated CA bases and with limited length (e.g., ssDNA-12) and of bare gold electrodes (only modified with MCH); the original data showing the influence of various assay conditions on the hydrolysis efficiency. This material is available free of charge via the Internet at http://pubs.acs.org.

References

(1) Lehman, I. R. *J. Biol. Chem.* **1960**, *235*, 1479-1487.

(2) Breyer, W. A.; Matthews, B. W. *Nat. Struct. Biol*. **2000**, *7*, 1125-1128.

(3) Lu, D.; Keck, J. *Proc. Natl. Acad. Sci.* **2008**, 105, 9169–9174.

(4) Lehman, I. R.; Nussbaum, A. L. *J. Biol. Chem.* **1964**, *239*, 2628-2636.

(5) Thomas, K. R.; Olivera, B. M. *J. Biol. Chem.* **1978**, *253*, 424-429.

(6) Brody, R. S.; Doherty, K. G.; Zimmerman, P. D. *J. Biol. Chem.* **1986**, *261*, 7136-7143.

(7) Viswanathan, M.; Lovett, S. T. *Genetics* **1998**, *149*, 7–16.

(8) Werle, E.; Schneider, C.; Renner, M.; Volker, M.;Fiehn, W. *Nucleic Acids Res*. **1994**, *20*, 4354-4355.

(9) Wang,Y.; Zhang, C. H.; Tang, L.J.; Jiang, J. H. *Anal. Chem*. **2012**, *84*, 8602−8606.

(10) Song, C.; Wang, G. Y.; Wang, H. Z.; Wang, Y. J.; Kong,D. M. *J. Mater. Chem. B*. **2014**, *2*, 1549–1556.

(11) Ma,F.; Yang,Y.; Zhang, C. Y. *Anal. Chem*. **2014**, *86*, 6006−6011.

(12) Zhao, X. H.; Gong, L.; Zhang, X. B.; Yang, B.; Fu, T.; Hu, R.; Tan, W. H.; Yu, R. Q. *Anal. Chem.* **2013**, *85*, 3614−3620.

(13) Zhu, Y. H.; Wang, G. F.; Sha, L.; Qiu, Y. W.; Jiang, H.; Zhang, X. J. *Analyst* **2015**, *140*, 1260–1264.

(14) Wei, Y. L.; Chen, Y. X.; Li, H. H.; Shuang, S. M.; Dong, C.;Wang, G. F. *Biosens. Bioelectron.* **2015**, *63*, 311–316.

(15) Wang, X. L.; Li, F.; Su, Y. H.; Sun, X.; Li, X. B.; Schluesener, H. J.; Tang, F.; Xu, S. Q. *Anal. Chem.* **2004**, *76*, 5605-5610.

(16) Xu,Y. Y.; Jiang,B. Y.; Xie, J. Q.; Xiang, Y.; Yuan, R.; Chai, Y. Q. *Talanta* **2014**, *128*, 237–241.

(17) Li, S. Y.; Li, R.; Dong, M. M.; Zhang, L.Y.; Jiang, Y.; Chen,L. J.; Qi, W.; Wang, H. *Sens. Actuators, B* **2016**, *222*, 198–204.

(18) Danesh, N. M.; Ramezani, M.; Emrani, A. S.; Abnous, K.; Taghdisi, S. M. *Biosens. Bioelectron.* **2016**, *75*, 123–128.

(19) Wen,W.; Hu, R.; Bao,T.; Zhang, X. H.; Wang, S. F. *Biosens. Bioelectron.* **2015**, *71*, 13–17.

(20) Zhao, Q. L.; Zhang, Z.; Xu, L.; Xia, T.; Li, N.; Liu, J. L.; Fang, X. H. *Anal. Bioanal. Chem.* **2014**, *406*, 2949–2955.

(21) Wang, H. B.; Zhang, H. D.; Xu, S. P.; Gan, T.; Huang, K. J.; Liu, Y. M. *Sens. Actuators, B* **2014,** *194,* 478–483.

(22) Wang, Q.; Jiang, B. Y.; Xie, J. Q.; Xiang, Y.; Yuan, R.; Chai, Y. Q. *Analyst* **2013**, *138*, 5751-5756.

(23) Wang, Q.; Jiang, B. Y.; Xu, J.; Xie, J. Q.; Xiang,Y.; Yuan,R.; Chai, Y. Q. *Biosens. Bioelectron.* **2013**, *43,* 19–24.

(24) Jiang, B. Y.; Wang, M.; Li, C.; Xie, J. Q. *Biosens. Bioelectron.* **2013**, *43*, 289–292.

(25) Wu, Z.; Zhen, Z.; Jiang, J. H.; Shen, G. L.; Yu, R. Q. *J. Am. Chem. Soc.* **2009**, *131*, 12325–12332.

(26) Lv, Y. Q.; Xue, Q. W.; Gu, X. H.; Zhang, S. Q.; Liu, J. F. *Analyst* **2014**, *139*, 2583–2588.

(27) Xue, Q. W.; Zhang, G.; Wang, L.; Jiang, W. *Analyst* **2014**, *139,* 3167–3173.

(28) Gong, X.; Zhou, W. J.; Chai, Y. Q.; Xiang, Y.; Yuan, R. *RSC Adv.* **2015**, *5*, 6100–6105.

(29) Wang, H. B.; Zhang, H. D.; Xu, S. P.; Gan, T.; Huang, K. J.; Liu, Y. M. *Sens. Actuators, B* **2014**, 194, 478–483.

(30) Fojta, M.; Kubicarova, T.; Palecek, E. *Electroanalysis* **1999**, *11*, 1005–1012.

(31) Jin, Y. *Anal. Chim. Acta*. **2009**, *634*, 44–48.

(32) Yu, H.-Z.; Luo, C. Y.; Sankar, C. G.; Sen, D. *Anal. Chem.* **2003**, *75*, 3902–3907.

(33) Steel, A. B.; Herne, T. M.; Tarlov, M. J. *Anal. Chem.* **1998**, *70*, 4670–4677.

(34) Peterson, A. W.; Heaton, R. J.; Georgiadis, R. M. *Nucleic Acids Res.* **2001**, *29*, 5163–5168.

(35) Ricci, F.; Lai, R. Y.; Heeger, A. J.; Plaxco, K. W.; Sumner, J. J. *Langmuir* **2007**, *23*, 6827–6834.

(36) Wang, J.; Rivas,G.; Jiang,M.; Zhang, X. J. *Langmuir* **1999**, *15*, 6541–6545.

(37) Korada, S. K. C.; Johns, T. D.; Smith, C. E.; Jones, N. D.; McCabe, K. A.; Bell C. E. *Nucleic Acids Res.* **2013**, *41*, 5887–5897.

(38) Watson, J. D.; Crick, F. H. C. *Nature* **1953**, *171*, 737.

(39) Wilkins, M. H. F.; Stokes, A. R.; Wilson, H. R. *Nature* **1953**, *171*, 738–740.

(40) Shchepinov, M. S.; Case-Green, S. C.; Southern, E. M. *Nucleic Acids Res*. **1997**, *25*, 1155–1161.

(41) Wong, E. L. S.; Chow, E.; Gooding, J. J. *Langmuir* **2005**, *21*, 6957–6965.

(42) Peeters, S.; Stakenborg, T.; Reekmans, G.; Laureyn, W.; Lagae, L.; Aerschot, A. V.; Ranst, M. V. *Biosens. Bioelectron.* **2008**, *24*, 72–77.

For TOC only
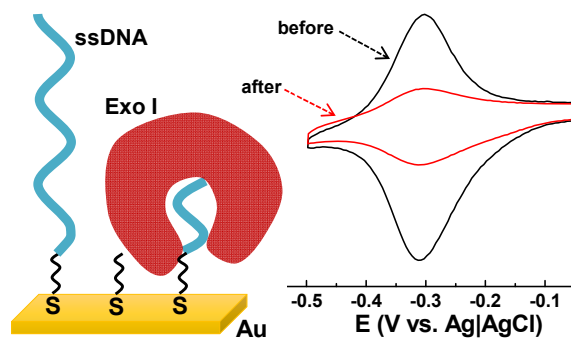
Supporting Information

for

Revealing and resolving the restrained enzymatic cleavage of DNA self-assembled monolayers on gold: electrochemical quantitation and ESI-MS confirmation

Xiaoyi Gao,[†] Mingxi Geng,[†] Yunchao Li[*,†], Xinglin Wang,[†] and Hua-Zhong Yu[*,‡]

[†]*Department of Chemistry, Beijing Normal University, Beijing 100875, P. R. China*

[‡]*Department of Chemistry, Simon Fraser University, Burnaby, British Columbia V5A 1S6, Canada*

* Corresponding authors: liyc@bnu.edu.cn,+86-10-5880-4077 (Y.L.); hogan_yu@sfu.ca, +1-778-782-8062 (H.Y.)

Additional experimental results include: the efficiency of repeated hydrolysis of ssDNA-48 and ssDNA-56 SAMs by Exo I (Figure S1); chronocoulometric (CC) study of the enzymatic hydrolysis of ssDNA SAMS with different chain lengths (Figure S2); comparison of the hydrolysis efficiency determined by CV and CC methods (Figure S3); CV study of the hydrolysis of ssDNA with repeated CA bases (Figure S4); ESI-MS characterization of the hydrolysis residues of ssDNA-48 SAMs (Figure S5); CV responses of the enzymatic hydrolysis of ssDNA-12 SAMs (Figure S6); CV responses of gold electrodes modified with MCH only with different concentrations of $[Ru(NH_3)_6]^{3+}$ (Figure S7); the original data showing the influence of various assay conditions on the hydrolysis efficiency of ssDNA-48 and ssDNA-56 SAMs (Table S1-S3).
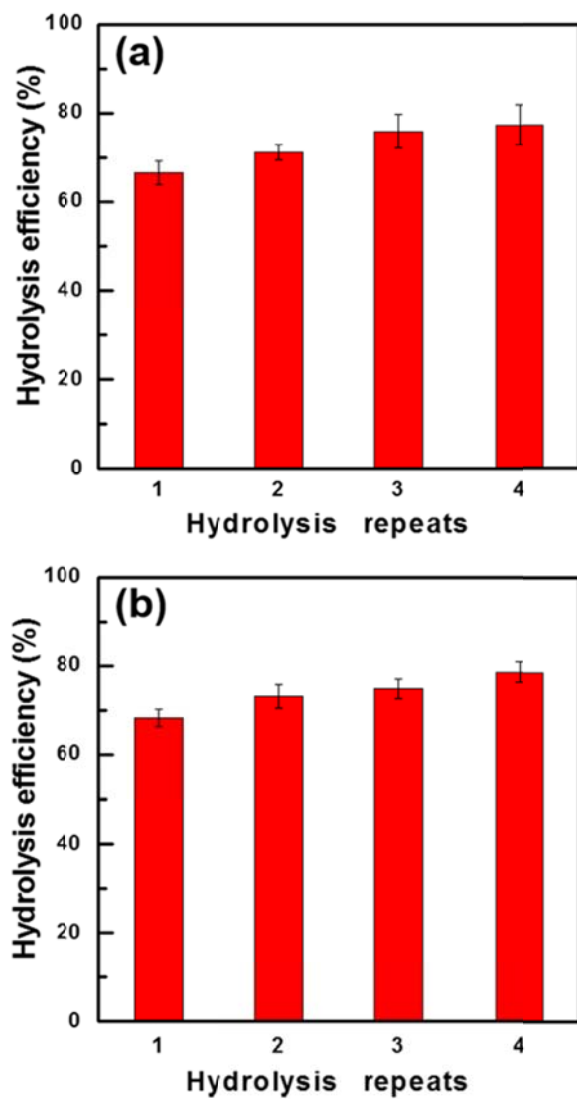
Figure S1. Hydrolysis efficiency of (a) ssDNA-48 and (b) ssDNA-56 SAM-modified gold electrodes after digested multiple times by 1.25 U/uL Exo I for 12 h at 37 °C.
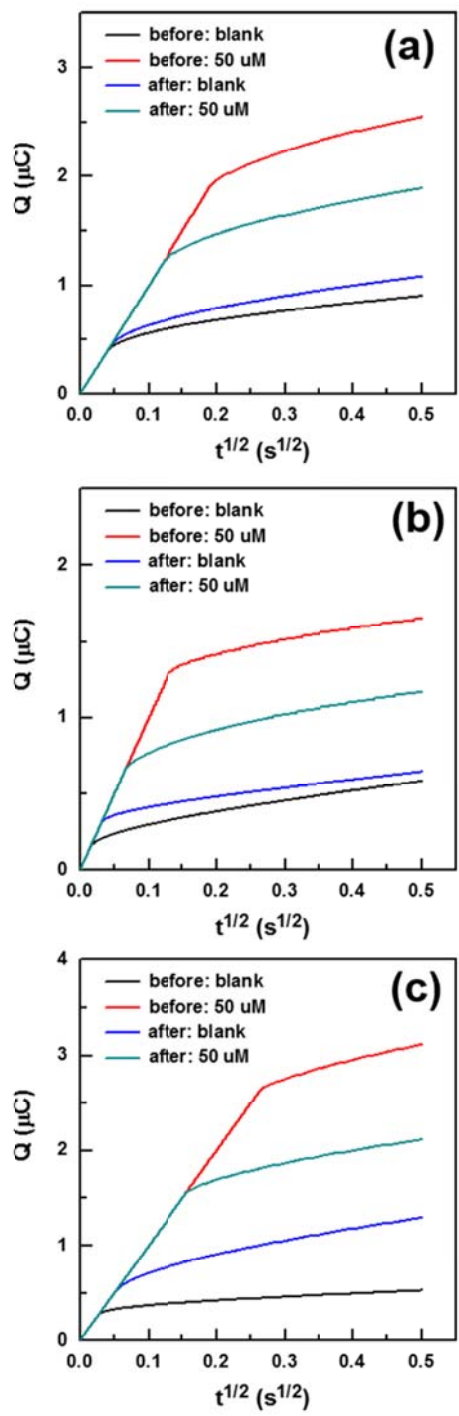
Figure S2. Chronocoulometric (CC) responses of gold electrodes modified with ssDNA-24 (a), ssDNA-48 (b), and ssDNA-56 SAMs (c) in 10 mM Tris buffer containing 50 μM $[Ru(NH_3)_6]^{3+}$; the electrode was subjected to 1.25 U/μL Exo I treatment for 12 h. The measurement was carried out with a pulse period of 500 ms and a pulse width of 540 mV (from + 40 mV to - 500 mV).
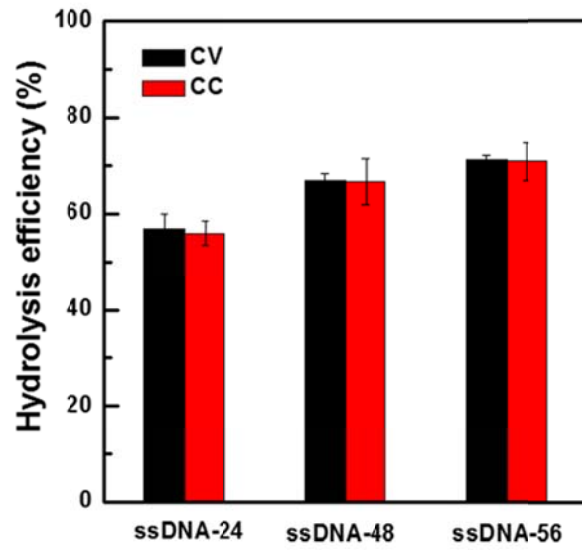
Figure S3. Comparison of the hydrolysis efficiency of surface-tethered ssDNA-48 determined by CV (black bars) and CC (red bars) method, respectively. The two sets of data are close to each other, which assures the validity of the CV determination discussed in the main text.
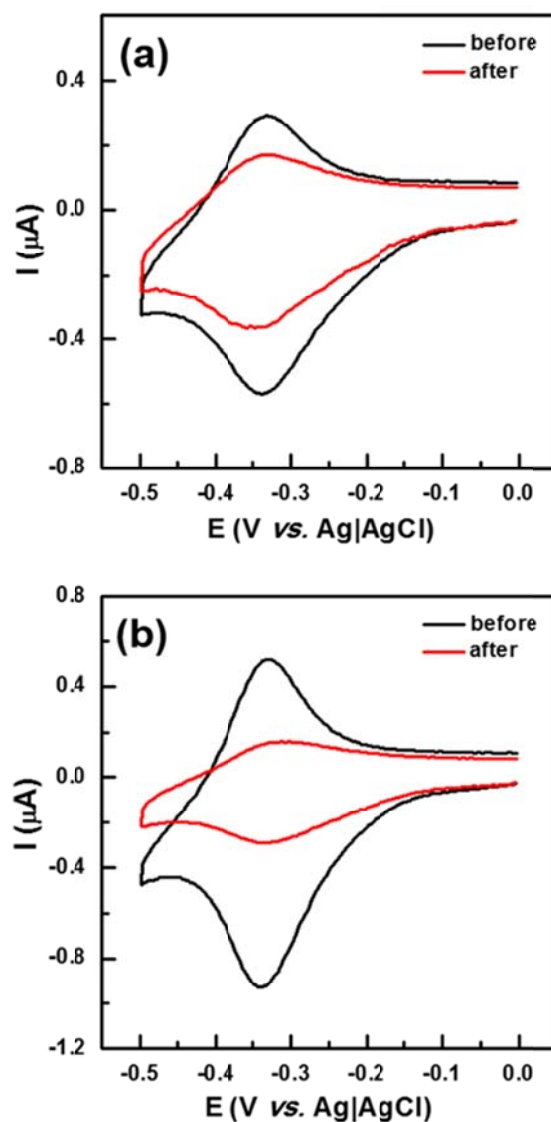
Figure S4. Representative CV responses of gold electrodes modified with ssDNA-48CA (a) and ssDNA-24CA (b) in 10 mM Tris buffer containing 5.0 μM $[Ru(NH_3)_6]^{3+}$ at 50 mV/s; the electrode was subjected to 1.25 U/μL Exo I incubation for 12 h. Thus determined hydrolysis efficiency shows no difference from ssDNA-48 and ssDNA-24 (respectively), indicating that the Exo I-catalyzed hydrolysis of ssDNA SAMs is not sequence dependent.
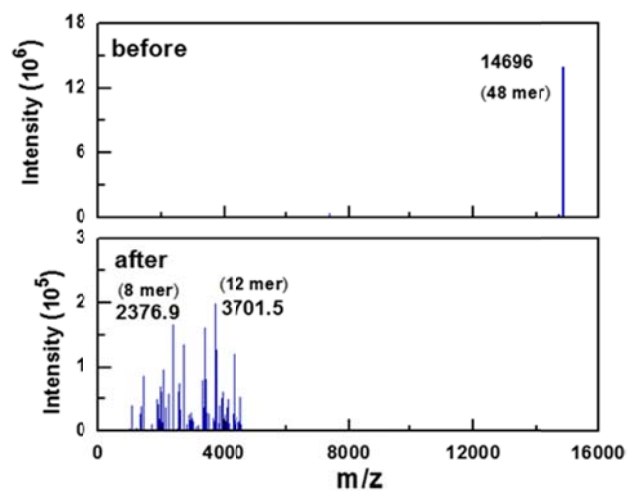
Figure S5. ESI-MS spectra of ssDNA-48 before and after hydrolysis with 1.25 U/μL Exo I at 37 °C for 12 h. The hydrolyzed DNA strands were removed from electrode surface by electrochemical reduction method; samples of multiple electrodes (> 40) were combined to achieve nM-concentrations for the ESI-MS measurements.
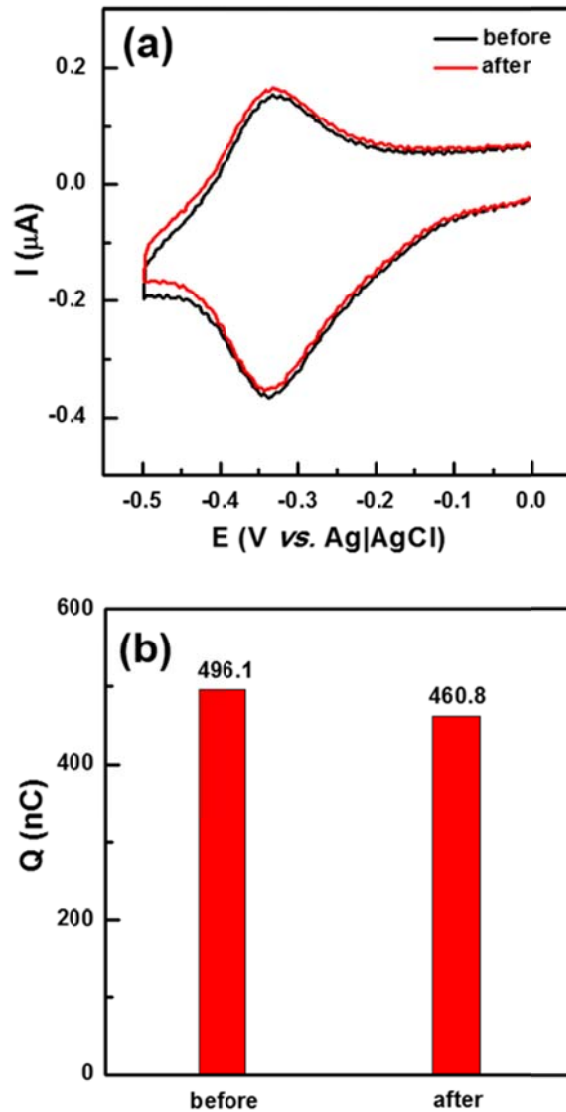
Figure S6. (a) Representative CVs of gold electrode modified with ssDNA-12 SAM in 10 mM Tris buffer in the presence of 5.0 μM $[Ru(NH_3)_6]^{3+}$ at 50 mV/s; the electrode was subjected to 1.25 U/μL Exo I and incubated for 12 h. (b) Comparison of the integrated charges (reduction peaks in (a)) of surface-tethered ssDNA-12 before and after the Exo I catalyzed-hydrolysis. It is clear that the hydrolysis is very low in this case, i.e., Exo I does not cleave surface-bound 12-mer ssDNA strands.

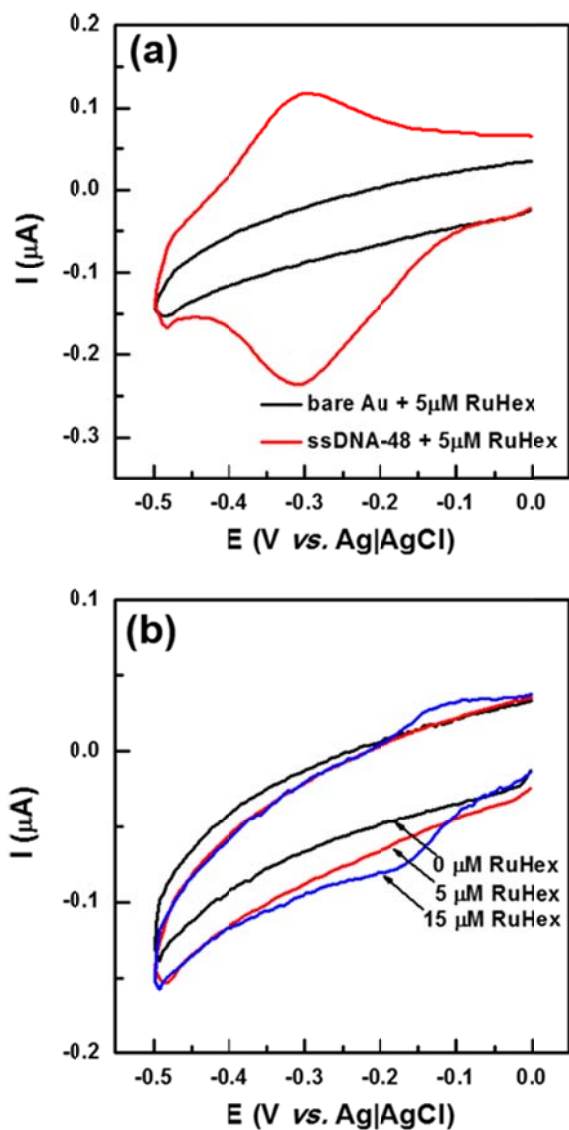**Figure S7.** (a) Representative CV responses of gold electrodes modified with ssDNA-48 (red curve) and MCH (bare gold, black curve) in 10 mM Tris buffer with 5.0 μM $[Ru(NH_3)_6]^{3+}$. (b) CV responses of gold electrodes modified with MCH ("bare gold") in 10 Tris buffer in the presence of different concentrations of $[Ru(NH_3)_6]^{3+}$. The scan rate is kept at 50 mV/s for all the measurements.

.

Table S1. Dependence of the hydrolysis efficiency of ssDNA-48 SAMs on the Exo I concentration

[Exo I] (U/µL)	Q_{int}/nC (before)	Q_{fin}/nC (after)	Hydrolysis efficiency (%)	Average±SD (%)
0	1391	1352	2.80	2.63±0.38
	1133	1108	2.21	
	1343	1304	2.90	
0.25	922.2	717	22.25	23.7±3.6
	1142	900.6	21.14	
	909.8	657	27.79	
0.625	1111	521.9	53.02	54.8±4.4
	952.1	461.7	51.51	
	964.3	387.6	59.81	
1.25	846.1	282.6	66.6	66.2±1.0
	884.6	309.6	65	
	889.8	294.6	66.94	
2.00	1139	375.9	67	67.4±0.6
	1094	349.3	68.07	
	1138	373.8	67.15	
2.50	990	368.6	62.77	65.1±3.4
	819.2	253.9	69.01	
	933.9	340.8	63.51	

Table S2. Dependence of the hydrolysis efficiency on the Exo I incubation time for ssDNA-48 SAMs on gold

Exo I incubation time (h)	Q_{int}/nC (before)	Q_{fin}/nC (after)	Hydrolysis efficiency (%)	Average±SD (%)
0.5	1063	919.6	13.49	14.6±1.8
	1128	940.5	16.62	
	1081	933.5	13.64	
1	1063	797.1	25.02	22.4±2.4
	1128	881.7	21.84	
	1081	862.0	20.26	
2	1063	511.1	51.92	56.8±4.2
	1128	466.3	58.66	
	1081	435.0	59.76	
3	1063	387.7	63.52	65.8±2.1
	1128	365.5	67.60	
	1081	362.0	66.51	
6	1063	351.0	66.98	65.9±0.4
	1128	373.8	66.86	
	1081	350.6	67.57	
9	1063	338.9	68.12	67.1±4.0
	1128	397.7	64.74	
	1081	294.9	72.72	
12	1063	355.0	66.60	68.3±2.6
	1128	323.2	71.34	
	1081	357.4	66.94	

Table S3. Correlation between surface density and hydrolysis efficiency of ssDNA-48 SAMs on gold

sample	ssDNA surface density (10^{12} molecules/cm^2)		Hydrolysis efficiency (%)	
	Surface density	Average±SD (%)	Hydrolysis efficiency	Average±SD (%)
1	3.33		65.60	
2	3.75	3.54±0.21	63.63	63.6±2.0
3	3.53		61.53	
4	8.85		67.05	
5	9.55	9.29±0.38	68.07	66.7±1.5
6	9.46		65.10	
7	11.15		69.70	
8	11.69	11.33±0.31	68.77	68.7±1.0
9	11.14		67.69	
10	12.06		71.04	
11	14.1	12.61±1.31	60.70	67.7±6.1
12	11.67		71.34	
13	14.47		60.62	
14	15.85	14.57±1.23	63.68	64.2±3.9
15	13.39		68.31	
16	18.18		74.90	
17	18.84	18.26±0.55	68.92	72.8±3.4
18	17.75		74.63	
19	20.38		68.68	
20	21.63	20.64±0.89	71.12	69.9±1.2
21	19.91		69.87	